

Large deformation analysis of buried pipelines

T. Koike, T. Imai & T. Kaneko
Kawasaki Steel Corporation, Tokyo, Japan

ABSTRACT: For the credible assessment of a seismic risk of the buried pipeline system, the crucial importance is laid on the accurate estimate of the pipe damage. This study presents a method of estimating a structural damage of buried pipeline when a severe earthquake causes permanent ground movement due to faulting, landslide, lateral spreading and liquefaction. To analyze the pipe deformation behavior caused by lateral differential ground movements, both of material and geometrical nonlinearities are taken into consideration. Final goal of this study is to propose a design methodology how to reduce structural damage of a pipeline network system which is buried in a potentially liquefaction-sensitive region.

1 INTRODUCTION

Buried pipelines are often damaged at mechanical joints, bent corners and connections with branches when a strong earthquake causes severe ground shakings (Shinozuka & Koike 1979).

More significant failures of the buried pipelines, however, appear in the liquefied ground where spatially extended large ground movements bring out not only the lateral bucklings and large deflections of small diameter welded pipes, but also the destructions of mechanical joints as reported in 1964 Niigata, 1989 Loma Prieta and 1990 Philippines Luzon Earthquakes.

Noting that the immediate restoration of lifeline after quake attack is primarily concerned especially not only in the residential area but also the highly congested business and industrial regions, the liquefaction-induced pipeline failures associated with their widely spreaded pipe damages must be prevented in order to minimize the occurrence of the malfunction of mutually interconnected lifeline systems.

The purpose of this study is

- (1) to develop the computer code to analyze the three-dimensional structural system of pipelines with material and geometrical nonlinearities against large ground movements;
- (2) to numerically assess the lateral buckling of buried pipelines to be caused in the liquefied ground; and
- (3) to propose a method how to reduce such buckling failures.

2 ANALYSIS

2.1 Structural model of buried pipelines

The pipeline network system includes not only straight and geometrical pipings, but also expansion joints, valves, manholes and structural facilities. Buried pipeline itself is modeled as a structural beam with perfect elasto-plastic stiffness, while several types of joint elements are modeled as spring elements. Rigid element model is also used for manhole and relevant building facilities which are supported with soil springs connected to their gravity centers.

Buried portion is characterized to be supported by the surrounding soils, which are modeled as ground stiffness. When the pipeline is deformed by liquefaction-induced lateral spreading, fault movement or landslide, the portion of the pipeline directly subjected to the relative soil movements is loaded by the soil, while other portions of the pipeline are restricted by their surrounding soil.

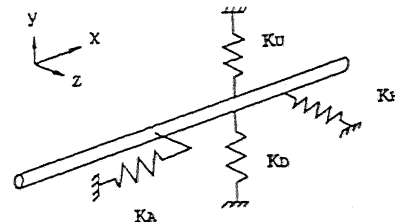


Figure 1. Idealized structural model of the buried pipeline and its surrounding soil

Soil-pipeline interaction is generally represented by components in the axial (or longitudinal) KA, transverse horizontal KH, and transverse vertical directions KU and KD (ASCE TCLEE 1984), as schematically shown by the springs. These effects can be simulated with mutually perpendicular bi-linear spring supports as shown in Fig.1.

2.2 Formulation

The structural analysis of pipeline systems is conducted on the basis of the conditions of continuity and balance of equilibrium at the nodal cross section for each segmented pipe element (Saleeb & Chen 1981). The finite element method is utilized herein to solve the stiffness matrices of the system, while geometrical and material nonlinearities are handled by application of a modified tangent stiffness approach.

The stress-strain relationship of the steel tubular pipe is assumed to be of the linear elastic and perfectly plastic type.

Beam element can be defined in the three dimensional local coordinate as shown in Fig.2 where the axial direction is identical to the x-axis, while the y and z axes are defined over the cross section of the beam element.

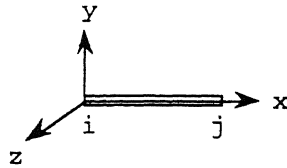


Figure 2. Local coordinate system of pipe element

The element stiffness matrix k_E of the individual beam element for the local coordinate is obtained by the combination of axial, bending and torsional stiffnesses.

Generalized cross sectional force p and its displacement u at the node i and j in Fig.2 are related with the element stiffness matrix k_E in the following equation.

$$\begin{bmatrix} p_i \\ p_j \end{bmatrix} = k_E \begin{bmatrix} u_i \\ u_j \end{bmatrix} \quad (1)$$

where p_i is the generalized force vector at the node i which includes the member force F and the bending moment M , while u_i is the generalized displacement u and the bending angle θ . p_i and u_i are given in the following forms.

$$p_i = \{F_x, F_y, F_z, M_x, M_y, M_z\}^T \quad (2)$$

$$u_i = \{u_x, u_y, u_z, \theta_x, \theta_y, \theta_z\}^T \quad (3)$$

and the element stiffness matrix are given by

$$k_E = \begin{bmatrix} k_o & -k_o \\ -k_o & k_o \end{bmatrix} \quad (4)$$

where

$$k_o = \begin{bmatrix} \frac{EA}{l} & 0 & 0 & 0 & 0 & 0 \\ 0 & \frac{12EI_y}{l^3} & 0 & 0 & 0 & \frac{6EI_y}{l^2} \\ 0 & 0 & \frac{12EI_z}{l^3} & 0 & -\frac{6EI_z}{l^2} & 0 \\ 0 & 0 & 0 & \frac{GK}{l} & 0 & 0 \\ 0 & 0 & -\frac{6EI_z}{l^2} & 0 & \frac{4EI_z}{l} & 0 \\ 0 & \frac{6EI_y}{l^2} & 0 & 0 & 0 & \frac{4EI_y}{l} \end{bmatrix} \quad (5)$$

in which $E, A, I_y, I_z, G, K, l, \nu, D_o, D_i$ are Young's modulus, cross sectional area, moment of inertia along y and z axes, shear modulus, Saint-Venant torsional rigidity given by $K = \pi(D_o^4 - D_i^4)/32$, length of pipe segment, Poisson ratio, external and internal pipe diameters.

For the bent pipe installed in the aboveground level, the flexibility analysis is utilized to obtain the stiffness matrix for the curved beam element in the following form:

$$k_E = \begin{bmatrix} Hf^{-1}H^T & -Hf^{-1} \\ -f^{-1}H^T & f^{-1} \end{bmatrix} \quad (6)$$

where f is the flexibility matrix to satisfy the relationship of $u_j^* = fp_j$ for elastic component u^* of bend pipe deformation and H is a matrix to release the rigid displacements u_i^* and u_j^* between the pipe ends i and j given by $u_j^* = H^T u_i^*$, while the force balance condition between p_i and p_j requires the equation:

$$p_i + H^T p_j = 0 \quad (7)$$

When the pipe beam is subjected to large axial force N_x and bending moments M_y and M_z , the stress distribution of the cross section exceeds from elastic level into partially plastic or fully plastic states.

Yield function (Usami et al 1990) is introduced for a tubular section of pipe subjected to axial load and bending moments as shown in Fig.3. These two curves in this figure are represented in the following equations:

$$\left(\frac{N_x}{N_p}\right) + \sqrt{\left(\frac{M_y}{M_y}\right)^2 + \left(\frac{M_z}{M_y}\right)^2} = 1 \quad (8)$$

$$\left(\frac{N_x}{N_p}\right)^{\beta_N} + \left\{\sqrt{\left(\frac{M_y}{M_p}\right)^2 + \left(\frac{M_z}{M_p}\right)^2}\right\}^{\beta_M} = 1 \quad (9)$$

where N_x and N_p are applied axial force and its yield force, M_y and M_z are applied bending moments, M_y and M_p are yield and fully plastic moments and β_N and β_M are control parameters for the yield function.

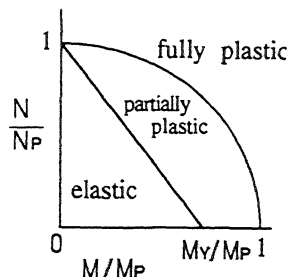


Figure 3. Yield function

Since the nonlinearity between structural strain and displacement must be considered for the large deformation behavior of the pipeline system, the geometrical stiffness matrix K_G is added to the corresponding elastic stiffness matrix K_E for the complete element assemblage so that the equilibrium equations for the system are

$$(K_E + K_G) U = P \quad (10)$$

in which U is a vector of the system global displacements and P is a vector of forces into the direction of the structural global displacements, and K_E and K_G are the structural stiffness matrices which is calculated by direct addition of the element stiffness matrices.

For the numerical analysis, tangent stiffness method is repeatedly applied until the residual balance of equilibrium is minimized.

3 SOIL SPRING

3.1 Spring modulus in the elastic region

The soil-pipeline interaction can be represented with the soil springs which must reflect the pipe dimensions and various surrounding soil properties. Several experimental results show the variation of these moduli dependent on the pipe diameter, the roughness of pipe surface and the degree of the soil compaction.

The current design guideline of water pipeline in Japan (JWWA) recommends to use the following relationship on the soil springs of K_A (axial component) and K_H (transverse horizontal component): $K_A=K_H=3\mu$ with shear modulus μ of the surrounding soil, while the guideline of the gas pipeline in Japan (JGA 1982) recommends to use $K_A=K_H=0.6\pi D$ with pipe diameter D which is estimated on the basis of experimental results for buried gas pipelines of the full-scale model.

Theoretical approach is often adopted to verify the applicability of the existing formula of these current definitions on spring moduli in water, oil and gas pipelines. Mutual comparisons between experimental results and theoretical ones were studied by the author (Koike 1983,1985) in which the analysis was developed on the elastic wave propagation theory for a straight pipe embeded in an infinitive elastic medium.

Table 1 is the definition of spring moduli used in the current design guideline, while the numerical results are summarized in Figs.4 and 5.

Table 1 The definition of spring moduli

Spring modulus	Analytical result	Japan Water Works Assn.	Japan Gas Assn. JGA
K_A	$K_A\mu$	3μ	$0.6\pi D$
K_H	$K_H\mu$	3μ	$0.6\pi D$

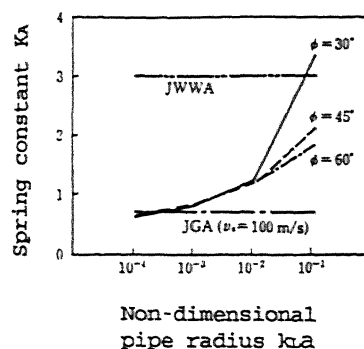


Figure 4. Spring modulus for axial pipe deformation vs. pipe radius for various incident angles of travelling seismic wave (a, k_L, v_s and ϕ are pipe radius, seismic wave number, shear wave velocity and incident angle)

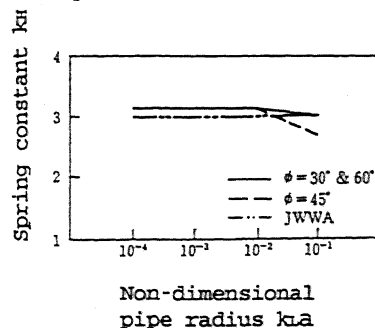


Figure 5. Spring modulus for bending deformation vs. pipe radius for various incident angle of travelling seismic wave

These figures imply that the good coincidence of the analytical result of KA with that of JWMA is observed for larger diameter pipe in Fig.4, while the same correspondence with that of JGA appears for smaller diameter pipe. Since the current formula of spring moduli represent good estimate with the analytical result for their familiar pipe dimensions, one may conclude that the current formula can be applicable in the elastic region.

3.2 Spring modulus in the inelastic region

It should be emphasized that the above discussion applies for the ground response excited by seismic wave propagation, where the ground strain is approximately less than 0.1% which cannot generate the pipe stresses exceeding the yield level (Shinozuka et al 1983). Those formula to be applicable in the elastic region of the soil may overestimate the axial and bending forces of the pipe when the lateral soil pressure are imposed on the pipe by relative displacement between the pipeline and its surrounding soil.

The transverse soil bearing force developed under high lateral pressure will affect the strains in pipelines subjected to large differential ground movement. The ultimate transverse soil forces per unit length P_u that can be developed for a buried pipe in sand can be expressed as

$$P_u = a P_o D \quad (11)$$

where P_o is effective overburden pressure, a is an empirical coefficient varying with pipe depth and the relative density of soil, and D is the pipe diameter. The corresponding critical displacement δ_u to P_u is given by $\delta_u = P_u / KH$.

The second stiffness for inelastic behavior of soil spring is assumed to be 1% of the original stiffness to be adopted in the following numerical calculations since there are no available data on the second stiffness.

4 NUMERICAL STUDIES

4.1 Comparison with experimental results

Numerical calculations were executed to estimate the accuracy of this method with the geometrical pipings such as bend and tee-junction. The analytical results are compared with the experimental data which were obtained in the field tests conducted by Japan gas association in 1982.

Pipe dimensions used in this experiment are summarized in Table 2.

Fig.6 represents the results of full-scale experiments and numerical analyses of buried

bend and tee-junction. Both results show good agreement in the pipe deformation and the force-displacement relationship over the inelastic region less than 5 to 8 times of δ_u .

Table 2. Pipe dimensions

Item	Unit	Value
Diameter	mm	318.5
Thickness	mm	6.4
Yield stress	kgf/mm ²	22.0
Ground stiffness		
axial	kgf/cm ²	33.4
horizontal	kgf/cm ²	68.5
vertical up	kgf/cm ²	68.5
vertical down	kgf/cm ²	68.5

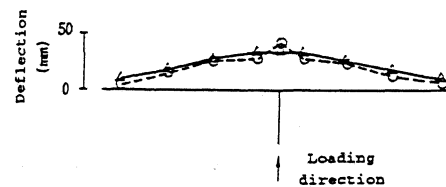
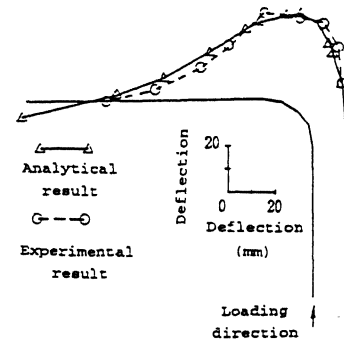
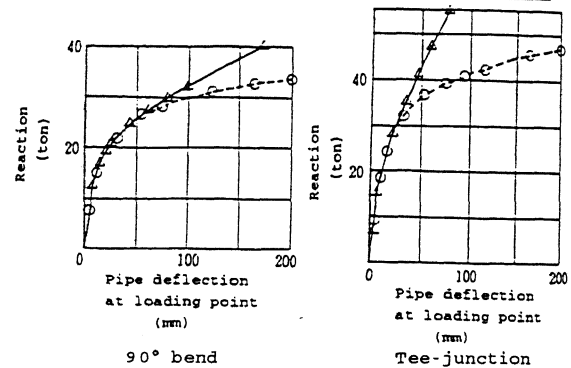


Figure 6. Comparison between the experimental results and numerical data of buried bend and tee-junction.

4.2 Pipe damage caused by large ground movement

Most significant damages of buried pipelines are often observed in the liquefied area after a severe earthquake in which the spatially extended large ground movements may cause tearing-off failure in tension or buckling failure in compression.

Photo 1 is an example of buckling failure of 150 mm diameter gas pipeline observed in the liquefied area in 1964 Niigata earthquake in Japan.

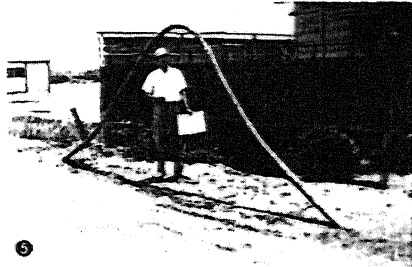


Photo 1. Buckled pipe in 1964 Niigata earthquake (reprinted from Wakamatsu 1991)

The following discussion is focussed on the pipe buckling behavior when axially forced displacement is subjected to the pipe embedded in the liquefied area. One may assume the values to be used in this calculation: pipe diameter=300mm, liquefied section=50m and deteriorated soil stiffness in the liquefaction area=1% of the original stiffness.

Fig.7 shows the effect of uplifting water pressure to initiate the lateral buckling when the ground displacement is axially forced in the compressive mode. The uplifting water pressure is obtained as the force resulting from pipe weight, floating force and excess pore water pressure in the liquefaction process.

In this figure, smaller uplifting pressure as $F=200\text{kgf/m}$ is not easy to initiate the lateral buckling up to the ground displacement of 9.6 cm,

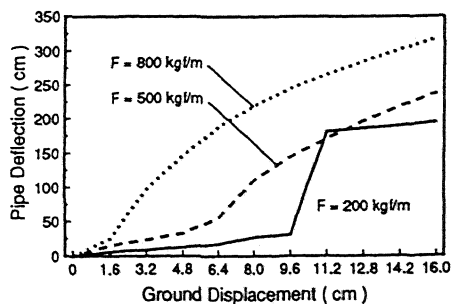


Figure 7. Buckled pipe deformations for ground movement under several uplifting water pressures

while larger uplifting pressure as $F=800\text{kgf/m}$ can cause the lateral buckling even in the small ground displacement of 1.6 cm.

Noting that most uplifting pressure is around $F=500\text{kgf/m}$, the ground displacement less than 10 cm may develop the same lateral buckling as shown in Photo 1.

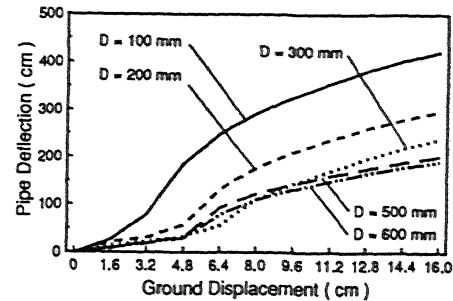


Figure 8. Buckled pipe deformation for ground movements under several pipe diameters

Fig.8 shows the effect of pipe rigidity fixed with $D/t=100$ when lateral buckling is induced by the ground movement together with the uplifting pressure of $F=500\text{kgf/m}$. One may find from this figure that smaller pipe is easily deflected than larger one.

Fig.9 reveals the effect of the surrounding soil restriction when the soil spring is deteriorated to be 1% or less of the original soil stiffness in the liquefaction process. According to this figure, large deterioration of soil stiffness during the liquefaction up to 1% or less can cause greater lateral buckling.

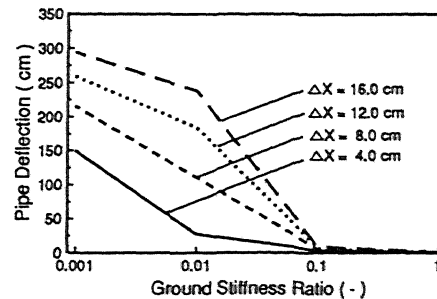


Figure 9. Effect of deteriorated restrictions of surrounding soil in the liquefied area

4.3 Partial soil improvement to protect the pipe uplifting

There are proposed many techniques and methods to protect structural failures when the spatially extended large ground movements are generated

in the liquefied area after a severe earthquake.

Fig.10 shows a model ground to resist the pipe uplifting due to the ground movement, in which a partial section with its interval of W is assumed to be replaced with the good soil free from the liquefaction, while L is the whole liquefied area.

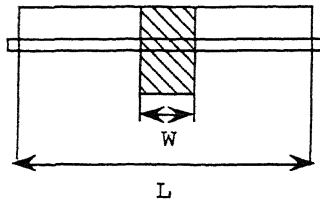


Figure 10. Analytical model

The analytical results in Fig.11 represent that the partial soil improvement is significantly effective to resist the pipe uplifting in the liquefied area. When W/L is 0.1 to 0.3, the lateral buckling deflection may be reduced to one-half or one-third of the deflection that appears in the pipe buckled in the aboveground.

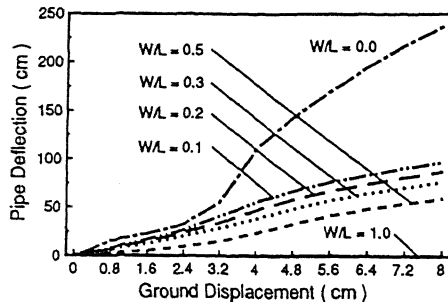


Figure 11. Effect of soil improvement to resist the pipe uplifting in the liquefied area

5 CONCLUSION

The proposed analytical procedure can evaluate the inelastic structural behaviors of the pipeline system to be caused by large differential ground movements on the basis of various nonlinear models in structural beam, soil springs, joint and rigid elements.

The following results can be summarized:

- (1) The computer code developed for the inelastic structural analyses of buried pipelines subjected to large ground movements can provide the good coincidence with the experimental results.
- (2) Small diameter pipeline can easily be deflected by the axial ground displacement, especially when the uplifting water pressure is large, or the surrounding soil

stiffness in the liquefied area is less than 1% of its original ground stiffness.

- (3) Partial soil improvement in the liquefied area is most effective to resist lateral buckling, even if the width of improvement area is 10 to 30 % of the whole liquefaction area.

Further studies will be required on the practical methods of anti-seismic countermeasures to reduce the pipe damages possibly to be suffered in the liquefied area, in which the weakest elements and/or the worst geometrical piping configurations in the spatially extended pipeline system must be surveyed.

REFERENCES

- ASCE TCLEE 1984. Guideline for seismic design of oil and gas pipeline systems, ASCE, pp.150-228.
- Japan Gas Association 1982. The seismic resisting design guideline of gas pipeline, JGA.
- Koike, T. 1983. Evaluation of structural strains of buried pipelines, Proceedings of structural engineering, JSCE, 331, pp.13-24
- Koike, T. 1985. Structural strains of the buried pipeline under seismic risk, Proceedings of the trilateral seminar-workshop on lifeline earthquake engineering, Taipei, Taiwan, pp.281-295.
- Saleeb, A.F. & W.F.Chen 1981. Elastic-plastic large displacement analysis of pipes, ASCE, Vol.107, No.ST4, pp.605-626.
- Shinozuka, M., H.Kameda & T.Koike 1983. Ground strain estimation for seismic risk analysis, ASCE, Vol.109, No.EM1, 1983, pp.175-191.
- Shinozuka, M. & T.Koike 1979. Estimation of structural strains in underground lifeline pipes, Lifeline earthquake engineering, ASME, PVP-34, pp.31-48.
- Usami, T. & T.Shibata 1990. Elastic-plastic large displacement analysis of steel framed structures with a stress resultant constitutive law, Proceedings of structural engineering, JSCE, 416, pp.339-348.
- Wakamatsu, K. 1991. Maps for historic liquefaction sites in Japan, Tokai University Press.